PREDICTING PHYSICAL PROPERTIES OF RESERVOIR ROCKS FROM THE MICROSTRUCTURAL ANALYSIS OF PETROGRAPHIC THIN SECTIONS

M.C. Damiani[*1], C.P. Fernandes[+2], A. D. Bueno[+3], L.O. E. Santos[+4], J.A.B. da Cunha Neto[+5], P.C. Philippi[+6•]

(*) Engineering Simulation and Scientific Software (ESSS)
Parque Tecnológico de Florianópolis - Rodovia SC 401 km 001
88030-000 Florianópolis, SC, Brazil

(+) Porous Media and Thermophysical Properties Laboratory (LMPT)
Mechanical Engineering Department. Federal University of Santa Catarina BP476
88040-900 Florianópolis, SC, Brazil.

Abstract

Important physical properties of petroleum reservoirs are, usually, obtained by applying standard experimental tests on rock samples collected along selected depths of the petroleum well. This is, presently, a laborious and high cost procedure. Present paper describes Imago, which is a new petrographic analysis software, developed for predicting the physical properties of reservoir rocks, starting from petrographic thin sections routinely produced in petroleum industry for microscopic analysis. Imago includes five main modules for i) segmentation of the porous phase from gray level and/or color digital images, ii) geometrical characterization of the porous microstructure, iii) three-dimensional reconstruction, iv) prediction of phase distribution in wetting-non wetting fluid equilibrium displacement and v) prediction of intrinsic permeability. Simulation results are compared with experimental results for Berea and some other petroleum reservoir sandstones.

---

[1] *Marcos Cabral Damiani is a software development engineer from the Engineering Simulation and Scientific Software (ESSS) staff. Presently, he is working in the software development of Imago at Porous Media and Thermophysical Properties Laboratory (LMPT).*

[2] *Celso Peres Fernandes is a Visiting Professor from Brazilian Petroleum Association (ANP), working at Porous Media and Thermophysical Properties Laboratory (LMPT). His fields of interest include image analysis and processing, 3D geometrical reconstruction and multiphase flow in porous media*

[3] *André Duarte Bueno has BS and MSc degrees in Civil Engineering. He is presently making his Doctoral studies in Porous Media and Thermophysical Properties Laboratory (LMPT) which includes equilibrium phase distribution and prediction of relative permeability in porous media.*

[4] *Luis Orlando Emerich dos Santos has a BS degree in Electrical Engineering and a MSc degree in Physics. He is presently making his Doctoral studies in Porous Media and Thermophysical Properties Laboratory (LMPT) which includes the use of lattice gas automata (LGA) for the analysis of single and two-phase flow displacements in 3D porous representations.*

[5] *José A. Bellini da Cunha Neto is Associate Professor at Federal University of Santa Catarina. He specializes in the macroscopic approach to fluid flow in porous media, image analysis and mercury intrusion processes.*

[6] *Paulo C. Philippi is Professor at Federal University of Santa Catarina where he heads the Porous Media and Thermophysical Properties Laboratory (LMPT). He specializes in image analysis and processing, single and multiphase flow in porous media and lattice gas automata (LGA) methods.*

• Corresponding Author (philippi@lmpt.ufsc.br)

1. Introduction

Important physical properties of petroleum reservoir rocks are, usually, obtained by applying standard experimental tests on rock samples collected along selected depths of the petroleum well. In addition to sampling costs, laboratory routine includes the manufacture of thin plates for petrographic analysis and the measurement of porosity, intrinsic and relative permeability and mercury intrusion tests, which are, presently, laborious and high cost procedures.

Recently, the advancement of image analysis methods, applied on thin sections of reservoir rocks, appears to open a promising fast and low cost technique for predicting these physical properties, from the solely knowledge of the porous microstructure of the reservoir rock. In this way, by using statistical homogeneity and spatial isotropy, the three-dimensional porous structure is supposed to be univocally related to two-dimensional representation obtained from thin plates. Furthermore, the physical properties of reservoir rocks, in petroleum extraction, are supposed to be given from the porous microstructure geometry and the physicochemical interaction between the involved fluids and the porous surface.

The main aim of porous media study is the description of equilibrium and transfer processes that are dependent on its porous structure. Common phenomenological methods use adjustable idealized models and/or experimental data to describe fluid occupation and the rates of fluid transfer. They are not able to explore local geometric information of the porous structure. Image analysis techniques, starting from gray-level and/or color pictures taken with an electron scanning and/or optical microscope of polished porous sections, are suitable to the analysis of the geometrical structure of porous media and could allow to the knowledge of their influence on fluid equilibrium and transfer. The main advantage of this approach is that the detailed knowledge of the porous structure enable to perform this study, starting from very fundamental physical laws *which are not dependent on the porous structure*.Virtual core analysis is a relatively recent research field and has been included in the SPE (Society of Petroleum Engineers) main research lines. At authors' knowledge, the only existing operational software developed to perform core analysis was constructed by Porous Media Research Institute (PMRI) (http://panda.uwaterloo.ca/pmri/) at Waterloo University and named VCLab (Virtual Core Laboratory). VCLab starts from binary segmented images and permeability calculations are based on percolation networks, obtained from the reconstructed three-dimensional representation.

Present paper describes Imago, which is a new petrographic analysis software, developed for predicting the physical properties of reservoir rocks, starting from petrographic thin sections routinely produced in petroleum industry for microscopic analysis.

Imago includes six main modules for:

i) filtering and segmentation of the porous phase from gray level and/or color digital images,
ii) geometrical characterization of the porous microstructure,
iii) three-dimensional (3-D) reconstruction,
iv) prediction of phase distribution in wetting non-wetting fluid equilibrium displacement including mercury intrusion,
v) prediction of intrinsic permeability based on skeleton method ,
vi) prediction of intrinsic permeability using lattice gas automata (LGA), by the integration of local velocity fields.

The segmentation module includes a neural network method for pattern recognition.

Geometrical three-dimensional reconstruction uses a new algorithm which starts from the measured porosity and autocorrelation function and uses a Fourier transform method for reducing processing time [1].

Phase distribution is predicted by supposing quasi-static displacement by a wetting and/or a non-wetting invader fluid into the porous structure [2].

Intrinsic permeability is predicted, in a first module, from the 3-D representation of the microstructural skeleton [3]. Another permeability module include, a boolean lattice gas automata (LGA) for predicting permeability by integrating the velocity field inside the three-dimensional representation of the porous structure.

Constructed in C++ object-oriented language to be a usable tool in petroleum engineering practice, Imago is multiplatform (Win32 and X-Window) and user-friendly, with tools for generating and visualizing intermediate results: lists, graphics and image properties, process log and status. Special tools for three-dimensional scientific visualization such as rendering, rotation, translation, zoom and two-dimensional cross-sections, are also provided.

Simulation results are compared with experimental results for Berea and some other petroleum reservoir sandstones.

2. Geometrical analysis and processing: filtering, segmentation and 3-D reconstruction

Imago was developed for predicting the physical properties of reservoir rocks, based on petrographic thin sections routinely produced in petroleum industry for microscopic analysis (Figure 1). Imago starts from color and/or gray level digital images, obtained after, respectively, optical and/or electron-scanning microscopy performed on reservoir rocks thin plates.

2.1 Filtering

Small features in the image are frequently found as the result of polishing procedures and/or image acquisition and appear as image noises. These noises are eliminated from the analysis by using spatial filters. The most commonly used filters are the *low-pass* filter, which attenuates color gradients and *median* filter that eliminates small discontinuities without any geometrical consequence.

2.2 Segmentation

For fluid flow simulation purpose, it is only necessary to segment the original digital image in solid and porous phases, resulting in binary black and white images. Thresholding is performed, by Imago, in accordance with the following methods.

2.2.1 Color images

Color digital images are derived from optical microscopy. Thin plates are prepared by introducing a colored resin into the porous structure and the porous phase is identified as the geometrical region related to the particular resin’s color. Digital images are frequently acquired and stored as 24 bits files in the RGB color model. In this model, each color is the result of a combination of components red, green and blue [4]. Imago presents two packages for color images segmentation. The first one works directly with RGB color model and the second one starts from HSI model, where the information of color is stored in the hue (H) component, while components S and I give information on saturation and intensity, respectively. Thresholding is performed using inter-class variance maximization method [5], applied to each component histogram in both color models. Taking petroleum industry needs, segmentation method was automated, although manual segmentation is also enabled in this module, when, due to polishing and/or acquisition problems, original digital image has not a good quality. In this way, *zoom*, *hand* and *preview* tools were included in this module to simplify manual segmentation work (Figure 2).

2.2.2 Gray-level images

Imago includes three gray-level segmentation modules. The first module is manual and based on the histogram threshold which appears to best separate the gray-level classes associated to solid and porous phase, respectively. The second module is automatic and based on the inter-class variance maximization method. The third module uses the global entropy method introduced by [6] and was, also, automated.

Imago also includes a neural network module for both gray level and color images that is, presently, in its developing phase. Preliminary results are very promising and the intention is to validate this method, which is very suitable for automating.

2.3 Measure of geometrical parameters

2.3.1 Autocorrelation function

In porous materials, one can theoretically distinguish between the solid and pore phase. The pore space of porous media can be characterized by the phase function Z**(x)** as follows:

$$Z(\mathbf{x}) = \begin{cases} 1 & \text{when } \mathbf{x} \text{ belongs to the pore space} \\ 0 & \text{otherwise} \end{cases} \tag{1}$$

where **x** denotes the position with respect to an arbitrary origin.

The porosity ε, the autocorrelation function C(**u**), and the normalized autocovariance function $R_Z(\mathbf{u})$ can be, respectively, defined by the following statistical averages (denoted by an overbar):

$$\varepsilon = \overline{\mathbf{Z}(\mathbf{x})} \tag{2}$$

$$C(\mathbf{u}) = \overline{Z(\mathbf{x})Z(\mathbf{x}+\mathbf{u})} \tag{3}$$

$$R_Z(\mathbf{u}) = \frac{\overline{[Z(\mathbf{x})-e]\cdot[Z(\mathbf{x}+\mathbf{u})-e]}}{(e-e^2)} \tag{4}$$

Porosity ε is obviously a positive quantity which is limited to the (0, 1)-interval. It can be shown that a function $R_z(\mathbf{u})$ is a normalized covariance function if all its Fourier components are nonnegative. This work is restricted to homogeneous media, where statistical parameters are assumed to be independent of position **x** in space. Thus, the porosity is constant and $R_Z(\mathbf{u})$ depends only upon the vector **u** being independent of position **x**. Moreover, when the porous media is isotropic, R_Z is a function of only $u = |\mathbf{u}|$, and does not depend on the direction of **u**.

A simple method to calculate the correlation function and normalized covariance function was used by [7], [8]. Let S be a section of a porous medium, given by a 2-D binary representation,

porous phase is represented in black and the solid matrix in white. The binary image S is divided into two halves S_1 and S_2. Hence,

$$S=S_1 \cup S_2,\ S_1 \cap S_2 = \varnothing \tag{5}$$

In order to calculate $R_z(u)$, S_1 is first translated by a distance u along the x-axis; yielding $S_1(+u)$. The spatial average indicated in Eq. (3) is calculated as an intersection of images,

$$\overline{Z(x,y)\cdot Z(x+u,y)} = S_1(+u) \cap S \tag{6}$$

giving the correlation function.

Since C(u) is related to the *probability* of finding two points separated by u and belonging to the same phase, it is, however, advantageous to calculate the autocorrelation function C(**u**) as a function of the two-dimensional vector **u** =(x,y) and, then, to take its mean value around a circle with radius $u=|\mathbf{u}|$. This last procedure produces more reliable C(u) values because it increases the number of realizations needed to calculate this probability. For an image f(x,y), the Fourier transform of the autocorrelation function is also the power spectrum of f(x,y) (Wiener-Khinchin theorem). The 2-D autocorrelation function is calculated in Imago by using the Fourier transform. Fluctuations are drastically reduced, when C(u) is calculated using Fourier transform.

In this way, with the Fourier transform of phase function, the correlation function can be obtained, rapidly, using Fourier transform methods. Figure 3 show, a surface display representation of the power spectrum of a porous section binary image. The correlation function is the inverse Fourier transform of the power spectrum.

Given the two dimensional estimate $C(x,y)$, we can obtain the desired one dimensional (isotropic) correlation function C(u) by averaging over the $C(x,y)$ values at a fixed radius u. Except for the cases (0,u) and (u, 0), $C(x,y)$ will not generally be known at the points of interest (see Figure 4).

Figure 5 shows the correlation function obtained with Fourier transform method, compared with the previous displacement method.

2.3.2 Pore Size Distribution

In Imago, pore size distribution of binary 2-D sections is obtained by successive *opening*, derived from mathematical morphology and using balls with increasing radius [5]. The resulting image can be viewed as the union of balls completely enclosed in the porous phase. Thus, after opening, porous phase lost all the features smaller than the opening ball. The cumulative porous distribution is, then, given by:

$$F(r) = \frac{e - e(r)}{e} \tag{7}$$

where e is the total porosity of the original image and $e(r)$ is the volume fraction of the porous phase after opening with a radius r ball.

To reduce time processing, opening operation is not applied directly to the binary image, but to a transformed image called background distance image**.** In this image, each pixel is labeled with the smaller distance from it to the neighbor background. This labeling technique uses a sequential algorithm [9], where the Euclidean distance is approximated by a discrete integer distance. The most commonly used discrete distance is the chamfer distance known as $d_{3\text{-}4}$, where each neighbor from a given point, taken following the horizontal and vertical coordinated axis, are considered to be 3 measuring units distant from the starting point. The diagonal neighbors are considered to be at 4 measuring units from that point. Thus, this discrete distance gives the numerical approximation of $4/3 = 1.333...$to the square root of 2 (1.4142...). The main advantage of using this discrete distance is related to the lower computer storage as only integers are stored in resident memory. Balls generated with $d_{3\text{-}4}$ distance that are used to perform opening operation are octagonal in shape.

2.4 Three-dimensional reconstruction

Three-dimensional reconstruction is based on a modification of Adler *et a*l. Gaussian truncated method [7] proposed by [1]. In Adler 's method, three-dimensional stochastic simulation of porous structure is based on the generation of a random non-correlated field X(**x**), which gives the correct binary phase function Z(**x**), after the successive application of a linear and a non-linear filters. Linear filter gives Y(**x**), which is a convolution

$$Y(\mathbf{x}) = a * X = \sum_{\mathbf{s}} a(\mathbf{s}) X(\mathbf{x}+\mathbf{s}) \tag{8}$$

inside a spherical domain with radius ℓ equal to the correlation length, measured at the original 2-D binary image. Non-linear filter transforms Y(**x**), which is a real variable field to a binary field $Z(\mathbf{x}) \in \{0,1\}$. By assuming homogeneity and isotropy, 3-D pore structure can thus be constructed from 2-D porous sections, preserving porosity and autocorrelation function. Another way to carry out linear filter is to generate Y(**x**) from X(**x**) using Fourier transform [10]. From a computational point of view, the use of the fast Fourier transform algorithm, instead of laborious solution of nonlinear equation, makes the Fourier transform superior to linear filter method. Further, although Fourier transform $\hat{a}(\mathbf{p})$ of a real field $\alpha(\mathbf{r})$ is complex, it can be easily show that in discrete representations, due to periodicity and conjugate symmetry properties of Fourier transform, computer resident memory requirements are the same for both fields. A truncated Gaussian method by using Fourier transform was proposed by [1]. The difference between this method and the previous ones is that the field Y(**x**) is directly generated from its autocovariance function $R_Y(\mathbf{u})$. In fact, by the Wiener-Khinchin theorem, the Fourier transform of the autocovariance of a function is the power spectrum of this function, i.e.,

$$\hat{R}_Y(\mathbf{p}) = \Im(R_Y(\mathbf{u})) = |\Im(Y)|^2 = \left|\hat{Y}\right|^2 \tag{9}$$

Therefore, if the autocorrelation function is known for an arbitrary field Y(**x**), Fourier transform can be used to generate this field, with the same autocorrelation function. In fact, the above equation means that the Fourier transform $\hat{R}_Y(\mathbf{p})$ of $R_Y(\mathbf{u})$ is only related to the magnitude $\left|\hat{Y}\right|$ of $\hat{Y} = \Im(Y)$. This means that the phase angle of $\hat{Y}$ does not depend on the autocovariance

$\hat{R}_Y(\mathbf{p})$, or, in other words, that any two functions, $\hat{Y}$, with different phase angle may give the same autocorrelation. This method does not need the linear filter and so avoids solving the nonlinear equations, reducing computer running time. Using the fast Fourier transform makes this algorithm more efficient. This idea was also used by [11] in reconstructing two-dimensional serial sections in their hybrid approach. However, their method needs linear filter to generate 3-D porous structure representations from these non-correlated serial sections. Present approach avoids solving a set of nonlinear equations associated with linear filter transform. In addition, when compared with Adler's method [10], it reduces the resident memory requirements, because the independent gaussian field data $X(\mathbf{x})$ are not needed. Therefore, both operating time and computer memory requirements are improved. These are the advantages of the truncated Gaussian method by using Fourier transform used by Imago.

Figure 6 shows a schematic description of Liang *et al.*'s method used in the reconstruction module of Imago and Figure 7 presents an example of output of this package, showing a comparison for the cumulative distribution of pore volume fraction between the values measured on the original binary image and the mean value obtained by measuring on several 2-D cross sections of the reconstructed microstructure.

Opening operation, section 2.3.2, was used in this computation step. Factor N is related to the linear size of the 3-D spatial representation and factor n is a sampling factor taken over $R_Z(u)$ data: sampling factor n means that the only points considered for $R_Z(u)$ data were the ones separated by n-1 pixels.

Results show that, when sampling factor n is reduced, three-dimensional reconstruction gives a systematic deviation with a larger amount of small size pores when compared to the original binary image. The better agreement was obtained, in present sample case, for n=5 and n=6. In fact, it must be remembered that present reconstruction method is based: i) on the hypothesis that the target original two-dimensional representation, is a realization of a stochastic process which is considered to be ergodic and stationary and ii) on the hypothesis that this process is Gaussian and can be, inherently, described by its only two first moments.

Imago has a three dimensional window for visualizing the three-dimensional reconstructed microstructure presented by iso-surfaces and/or iso-lines, with important operational tools including orthogonal cuts, zoom, translation and rotation. Figure 8 shows an example of this software's feature.

3. Prediction of phase distribution in immiscible displacement

Determination of phase distribution inside the porous structure is an important problem in oil recovery, giving reliable information for the prediction of recovery ratio and rate on secondary extraction.

Imago's package for the prediction of phase distribution is based on [2], [12]. Phase distribution is simulated by supposing that equilibrium states are attained through quasi-static processes. Method is based on the relationship between capillary pressure and the curvature radius of the interface given by Young-Laplace's equation, when this interface is supposed to be spherical:

$$r^i = \left| \frac{(d-1)\sigma_{AB}}{P_{A_o^i} - P_{B^i}} \right| \qquad (10)$$

where d is the Euclidean dimension of the space, σ_{AB} is the interfacial tension between fluids A and B, $P_{A_o^i}$ is the pressure at the domain of fluid A which is connected to a free region L, and P_{B^i} is the pressure of fluid B, at step i.

In this way, for a given capillary pressure $P_{A_o^i} - P_{B^i}$, non-wetting phase will be found in the geometrical region where it is possible to be place a ball with radius r^i, given by the above equation, and problem is reduced to a geometrical problem that can be solved by image analysis methods. Method is fully described in [2], [12] and readers are referred to these papers for further details.

Imago's 3-D visualization window enable the software operator to follow fluid displacement in the course of invasion process. An example of such a visualization is given in Figure 9 showing, wetting fluid location in an imbibition process, at an intermediate pressure step.

3.1 Mercury intrusion simulation

Mercury intrusion on samples of reservoir rocks is a routinely performed experimental test in petroleum industry, giving information on porosity, size distribution of pore constrictions and thresholding constriction diameter.

Imago's package for the simulation of mercury intrusion is the same used for the prediction of phase distribution explained above considering a quasi-static displacement of non-wetting fluid into a reconstructed porous structure, initially filled with an ideally compressible fluid. Contact angle with respect to non-wetting fluid is further corrected from the 180^o value, used in the simulation, to the 140^o value that is commonly accepted between experimenters.

Figure 10 gives a comparison of simulation results with experimental results for Berea500 sandstone. Best sampling factor was n=5. For testing statistical homogeneity, simulation was performed for three different linear sizes: N=60, 80 and 100.

4. Flow simulation

4.1 Intrinsic permeability

The simplest approaches for the calculation of intrinsic permeability, based on the idea of conduit flow, ignore the fact that different pores are interconnected with each other. These are called capillary permeability models, among which the so-called Carman-Kozeny model enjoys much greatest popularity. Another permeability model is the cut-and-random-rejoin model. The sample is sectioned into two by a plane perpendicular to the flow direction, and the two parts are rejoined together in a random fashion. The flow rate in the capillaries is assumed to be described by a Hagen-Poiseuille relationship. In empirical permeability models permeability is usually correlated with some characteristic parameters. Network models have been used in the last four decades. The simplest network is a regular lattice, which consists of a regular arrangement of sites or "pores", connected by bonds or "throats". Pores and throats are characterized by their radii, with an independent probability distribution function for each, and by the center-to-center distance. Furthermore, the lattice is characterized by its coordination number, the number of throats meeting at a pore. Regular networks such as square, hexagonal, kagomé, trigonal, cube, and cross square were treated. Network models are all based on the some information of pore structure, such as pore size distribution and coordination numbers. But, these data are almost assumed in the previous works.

Imago has two packages for permeability calculation. The first package is based on the Skeleton Method and the second one is based on a Lattice Boolean Model.

4.2 Skeleton Method

Imago uses skeleton method [3], where a detailed analysis and validation results can be found. The skeleton of a porous structure is a connected line composed by all points p that are equally distanced from porous surface. In this way, it can be considered as the line giving a first approximation to the *main flow line* through the porous structure. Skeleton is, thus, an intermediate level model, between permeability models based on percolation networks and models based on the integration of local velocity fields. In this way, considering, in addition, the meaningless of *secondary flows* for the calculation of fluid transfer rate, in low Reynolds number flows, Imago calculation method is based on the following assumptions:

i) Skeleton nodes are considered as flow bifurcation points;
ii) Flow between two successive nodes is considered to be one-dimensional, through a variable area cylindrical duct.

The reconstructed 3-D porous structure is usually a cube with side length $L_x \times L_y \times L_z$. The x-axis of the medium is chosen to be parallel to the direction of macroscopic flow. Impervious boundary conditions are applied to the external surfaces of the cube that are parallel to axes y and z. The skeleton of the pore structure is obtained by using Ma's thinning algorithms [3]. The 3-D skeleton of pore structure provides a real network. The hydraulic conductance of the fluid in the network can be calculated from the local hydraulic radius. Therefore, permeability can be estimated from the above data.

To compute intrinsic permeability, we need to define the hydraulic conductance of the fluid in the network. Flow is assumed to be sufficiently slow. For each point p in a given link, there is associated a pore section in a plane which contains p and is orthogonal to the link. This section is obtained by performing an oblique slice of unity thickness in the reconstructed 3-D structure, orthogonal to the link. Furthermore, one makes the simplification that the resistance to fluid flow in the link point p may be characterized in terms of the hydraulic radius r_H of this pore section:

$$r_H = \frac{\text{area of cross section}}{\text{length of perimeter of cross section}} \tag{11}$$

Thus, the conductance of a fluid in a point of pore link, g_L, is given by Poiseuille's equation and may be written as:

$$g_L(p) = \frac{2\pi r_H^4}{\eta l} \tag{12}$$

where η is the fluid viscosity and l is the length of the pore (here l =1).

The overall resistance to flow between the two neighboring nodes i and j, is

$$\frac{1}{g_{ij}} = \sum_{p=i}^{j} \frac{1}{g_L(p)} \tag{13}$$

The flow rate of fluid between the two nodes,

$$Q_{ij} = g_{ij}(P_i - P_j) \tag{14}$$

where P_i and P_j are the nodal pressures. Since the fluid is incompressible, mass conservation requires that

$$\sum_j Q_{ij} = 0 \tag{15}$$

where j runs over all the links connected to node i. Equation (15) together with the appropriate boundary conditions form a complete solution to the steady flow of an incompressible fluid in the pore skeleton network. The equations are solved using successive over-relaxation:

$$P_i = \beta \frac{\sum_j g_{ij} P_j}{\sum_j g_{ij}} + (1-\beta) P_i \tag{16}$$

where β is a relaxation parameter.

By imposing a pressure drop ΔP across the skeleton network and computing the resulting single phase flow rate Q, the intrinsic permeability k of the pore network is calculated from Darcy's law:

$$k = \frac{\eta L Q}{A \Delta P} = \frac{\eta L_x Q}{L_y L_z \Delta P} \tag{17}$$

where Q is the volumetric flow rate, A is the normal cross-sectional area of the sample, L is the length of the sample in the macroscopic flow direction, $\Delta P \equiv P_1 - P_2$ is hydrostatic pressure drop, and η is the viscosity of the fluid.

To illustrate the process to calculate permeability, a 2-D skeleton of the pore space is shown in Figure 11, calculated at each porous point, by solving Stokes equations (Present paper used a lattice-Boltzmann method for the calculation of full velocity field).The links and nodes of the graph are, respectively, composed of points with exactly two neighbors and three or more neighbors. Dead ends are associated with stagnated flows and are eliminated from the skeleton. Figure illustrates a detailed porous region showing the skeleton superposed to the local velocity field, and depicts a geometrical region where flow is stagnated, presenting a low speed vortex. It is seen that, although, with a strictly geometrical background, skeleton method *can capture* stagnation regions by associating dead-ends in the geometrical description of these regions.

Table 1 gives a sample of validation result for Berea sandstone with a nominal permeability of 500 mD. Best results where found for sampling factors n=5 and n=6 which corresponds to the sampling factors giving the best agreement for pore size distribution (see Figure 7).

As secondary flows associated to flow deviations inside complex porous structures do not significantly contribute to the main flow resistance when the Reynolds number is very low, the present method appears to be very suitable and easier to use when compared with methods based on numerical solutions of Stokes equation, giving the full velocity field. In addition, it does not suffer

from the well-known limitations of methods based on percolation networks. In fact, the skeleton is constructed trying to preserve the fine details of the pore structure along the flow path and can, thus, better describe its influence on main flow.

4.3 Lattice Gas Cellular Automata Model

Imago includes a package for predicting intrinsic permeability of porous media based on Lattice Gas Cellular Automata (LGA) methods. Details about the model and validation results are given in [13], a companion paper submitted to present meeting. LGA is a relatively recent method developed to perform hydrodynamic calculations being object of considerably interest in the last years. The method is due originally to Frish, Hasslacher and Pomeau, [14]. In its simplest form, it consists of a regular lattice populated with particles that hop from site to site in discrete time steps in a process, often, called *propagation*. After propagation, the particles in each site interact with each other in a process called *collision*, in which the number of particles and momentum are preserved. An exclusion principle is imposed in order to achieve better computational efficiency.

In despite of its simplicity, this model evolves in agreement with Stokes equation for low Mach and low Reynolds numbers. Some aspects make LGA methods very attractive for simulating flows through porous media. In fact, the method is explicit in time and boundary conditions in flows through complex geometry structures are very easy to describe in LGA simulation. Simulations are performed with integers, needing less resident memory capability and boolean arithmetic reduces running time. LGA is, furthermore, very suitable for parallel processing.

Taking into account the above features, LGA model was introduced as a package of Imago software:

i) to increase the precision in permeability calculations, using a model based on the full velocity field,
ii) for validation purposes in the construction of simpler (and faster) permeability models.

Figure 12 shows a typical output from Imago's LGA package for the prediction of a Brazilian sandstone intrinsic permeability. Figure also shows pore size distribution measured as the mean from 10 original 2-D binary image, compared with the mean value obtained by measuring on several 2-D cross sections taken from the reconstructed microstructures. Sampling factor that gave the best agreement for pore size distribution was n=5, which was taken as a pattern value for the simulation with LGA model on reconstructed microstructures. Experimental permeability value was k=441 mD. Predicted permeability value was k=368 mD for a reconstructed porous structure with linear size N=100 and sampling factor n=5 and k=462 mD for N=200 and n=5. In fact, in addition to sampling factor, the correct choice of linear size N is important to ensure statistical homogeneity in permeability calculations. In general, statistical homogeneity in flow calculations is, only, ensured, at a linear size N that is, often, greater than the value that assures geometrical homogeneity in the calculation of pore size distribution. Further validation results can be found in [13].

5. Conclusions

Prediction of physical properties of reservoir rocks needs the correct knowledge of their three-dimensional porous structure and the correct understanding of fluids behavior inside porous space and of its physicochemical interaction with solid surfaces. These are, yet, very difficult and actual problems, which call for a very intensive research work.

This paper presented Imago, a new petrographic analysis software that includes very recent analysis methods, derived from geometrical stochastic analysis and fluid mechanics, intended to be a usable tool in petroleum industry.

Imago includes as it main new features:

i) a fast algorithm for three-dimensional geometrical reconstruction based on Fourier transform, with optimized computer resident memory storage requirements;
ii) a fast skeleton method for predicting intrinsic permeability, avoiding the well-known limitations of percolation networks;
iii) a very precise method based on lattice gas cellular automata for the prediction of intrinsic permeability, calculated from the integration of full velocity field inside porous space.

All these methods were integrated in a single software written in C++ object oriented language and based on a multiplatform library (Win32 and X-Window) which enables Imago to be run in a very large class of computers, ranging from the very diffused personal computers to high-level Unix-based workstations. A very elaborated graphical interface with on-line output windows, hand tools, lists, export/import modules and 3-D visualization make Imago user-friendly and flexible.

Validation results were also presented for Berea and some brazilian sandstones, including pore size distribution, mercury intrusion and intrinsic permeability.

Acknowledgements

The authors would like to thanks CENPES/PETROBRAS (Centro de Pesquisas e Desenvolvimento Leopoldo A. Miguez de Mello) for providing the images and experimental data of reservoir rocks. C.P. Fernandes gratefully acknowledges financial support of ANP (Agência Nacional do Petróleo).

References

[1] Liang, Z. R., Fernandes, C.P., Magnani, F.S. & Philippi, P.C., 1998, *A Reconstruction Technique of 3-D Porous Media by using Image Analysis and Using Fourier Transform*, **Journal of Petroleum Science and Engineering, 21**, 3-4, 273-283.

[2] F.S. Magnani P.C. Philippi, Liang Z.R. & C.P. Fernandes, 2000, *Modelling two-phase equilibrium in three-dimensional porous microstructures*, **International Journal of Multiphase Flow, 26** (1)**,** 99-123**.**

[3] Z.R. Liang, P.C. Philippi, C.P. Fernandes, and F.S. Magnani, 1999, *SPE Paper 56006: Prediction of Permeability From the Skeleton of 3D Pore Structure*, **SPE Reservoir Evaluation & Engineering, 2** (2), 161-168 .

[4] Gonzalez, R. C., Wood, R.E. (1992) ***Digital Image Processing***, Addison-Wesley Publishing Company.

[5] Coster, M. and Chermant, J.L., 1989, ***Precis D'analyse D'images***. Presses du CNRS, Paris.

[6] Kapur, J.N., Sahoo D.K., Wong A.K.C., 1981, A New Method for Gray Level Picture Thresholding using the Entropy of the Histogram **Computer Graphics, Vision and Image Processing 29**, 273-285.

[7] Adler, P.M., Jacquin C.G. and Quiblier J.A., 1990. *Flow in Simulated Porous Media*. **Int. J. Multiphase Flow**, 16: 691-712.

[8] Philippi, P.C., Yunes, P.R., Fernandes, C.P., Magnani, F.S., 1994, *The Microstructure of Porous Building Materials: Study of a Cement and Lime Mortar*, **Transport in Porous Media**, **14**, 219-245

[9]. J. M. Chassery, A. Montanvert, ***Géometrie Discrète en Analyse d'Images***, Editions Hermes, Paris, 1991.

[10] Adler, P.M., 1992. ***Porous Media: Geometry and Transports***. Butterworth-Heinemann, New York.

[11] Ioannidis, M.A., Kwiecien M. and Chatzis I., 1995. Computer Generation and Application of 3-D Model Porous Media: From Pore-Level Geostatistics to the Estimation of Formation Factor. **Paper SPE 30201 presented at the Petroleum Computer Conference, Houston, TX.**

[12] P.C. Philippi, F. S. Magnani and A.D. Bueno *Two Phase Equilibrium Distribution in Three-Dimensional Porous Microstructures***. Submitted to Produccion 2000 / Aplicaciones de la ciencia en la ingeniería de petróleo,** May 08-12 /2000, Foz de Iguaçu.

[13] L.O. E. Santos, P.C. Philippi, M.C. Damiani**.** *A Boolean Lattice Gas Method for Predicting Intrinsic Permeability of Porous Media.* **Submitted to Produccion 2000 / Aplicaciones de la ciencia en la ingeniería de petróleo,** May 08-12 /2000, Foz de Iguaçu.

[14] Frisch, U., Hasslacher B., Pomeau Y., 1986, *Lattice-Gas Automata for the Navier-Stokes Equation,* **Physical Review Letters, 56**, 1505-1508.

Figures and Tables

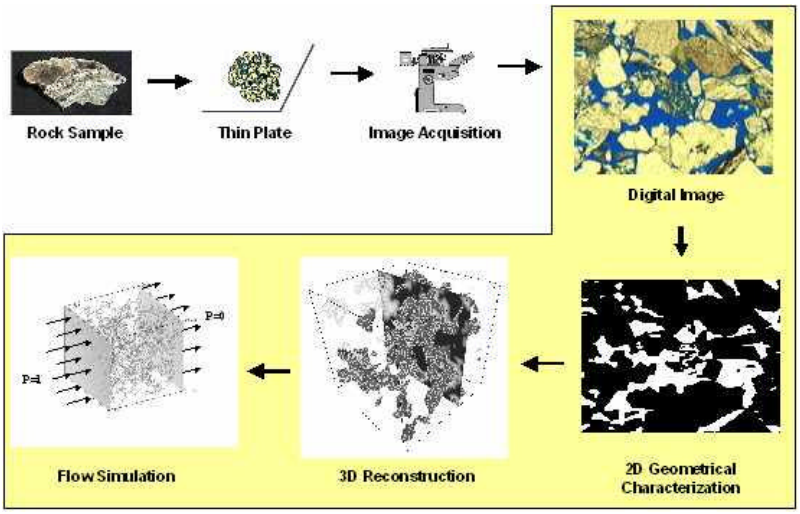

Figure 1. Imago methodology.

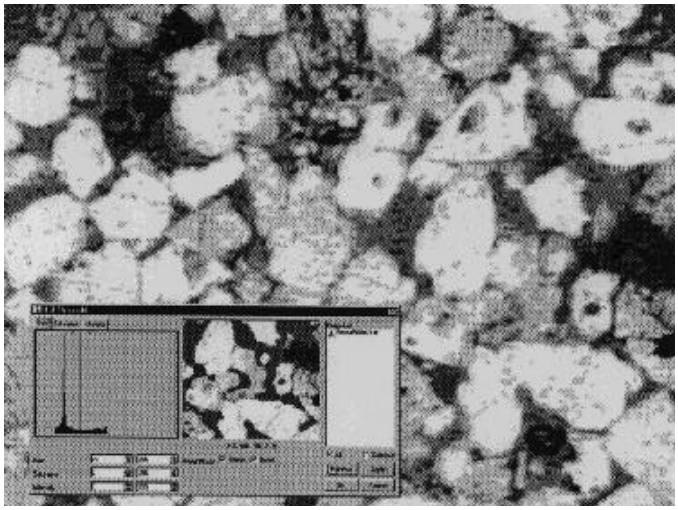

Figure 2. HSI segmentation module for color images.

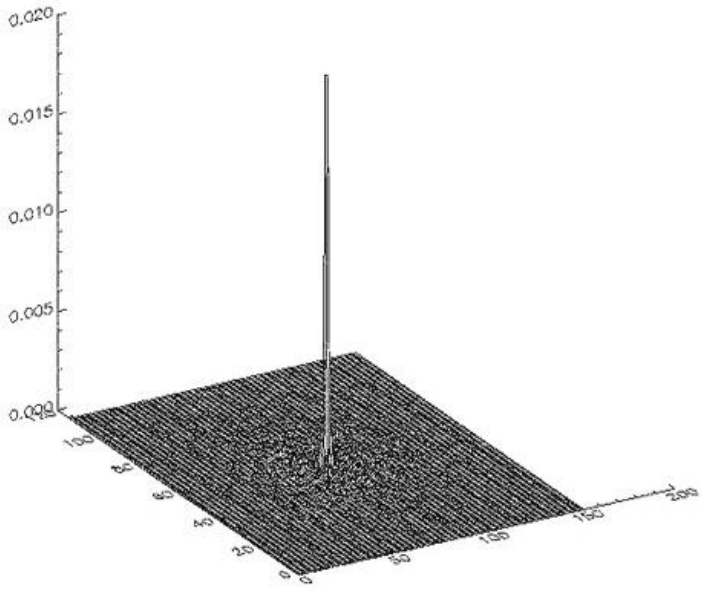

Figure 3. Surface display of power spectrum for a porous section binary image.

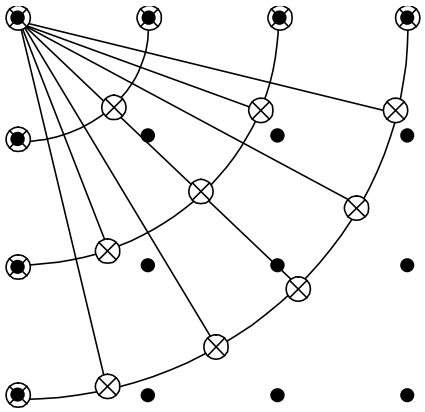

Figure 4. Obtaining the isotropic correlation function from discrete values for a particular image.

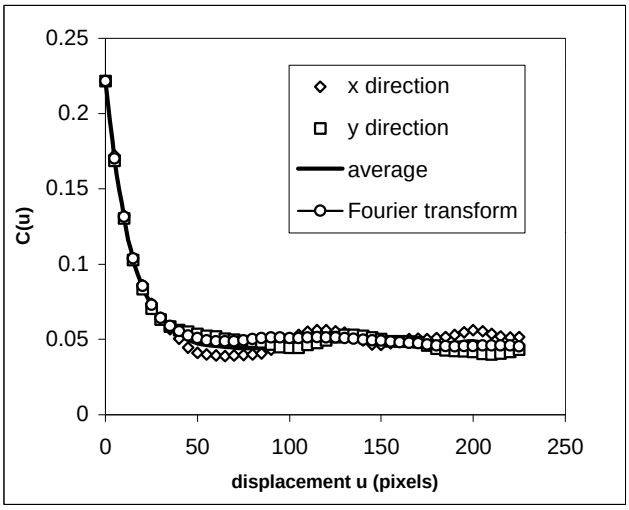

Figure 5. Comparison of correlation function.

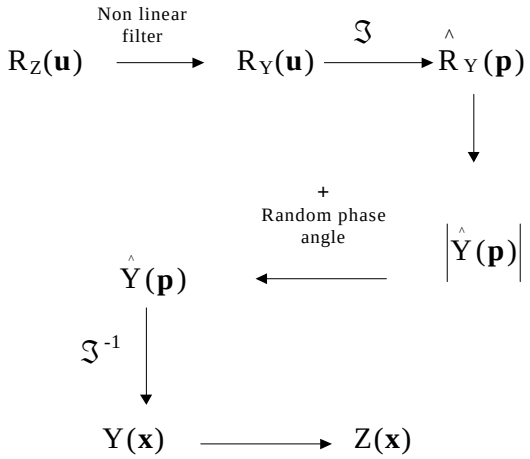

Figure 6. Schematic description of Liang et al.'s method for 3D reconstruction [1].

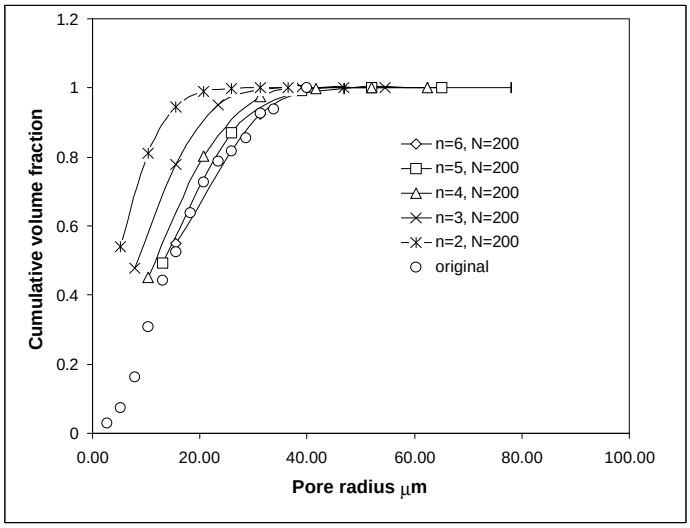

Figure 7. Comparison for the cumulative distribution of pore volume fraction of Berea sandstone 500mD, between values measured on the original binary image and the mean value obtained by measuring on several 2-D cross sections of the reconstructed microstructure.

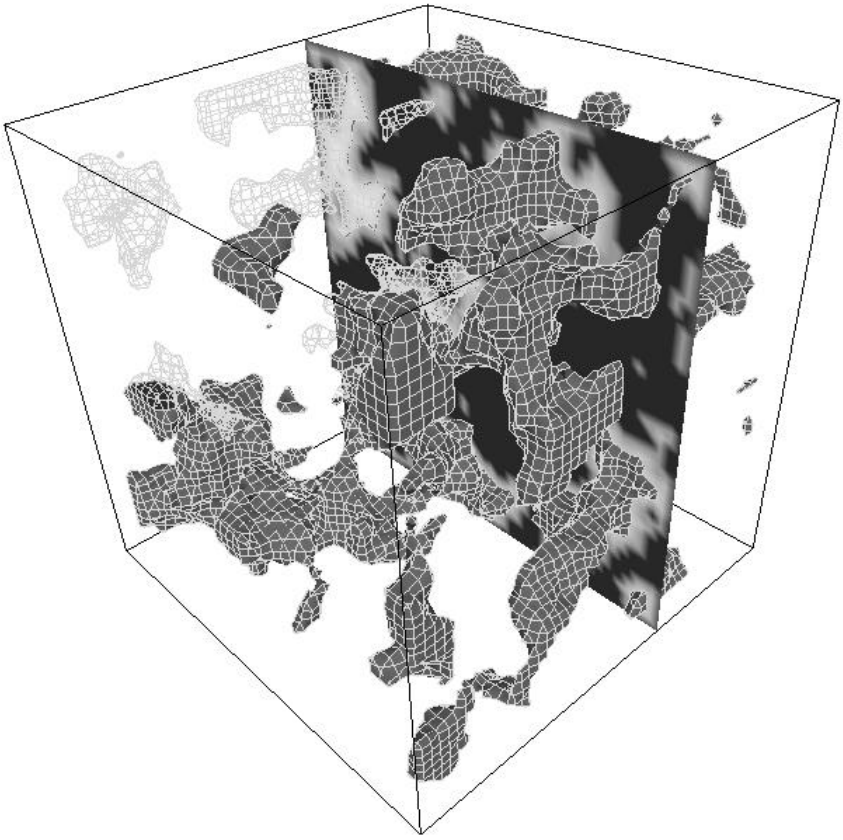

Figure 8. Imago three-dimensional visualization window.

Figure 9. Simulation of wetting-fluid invasion (in light) into a reconstructed 3D structure.

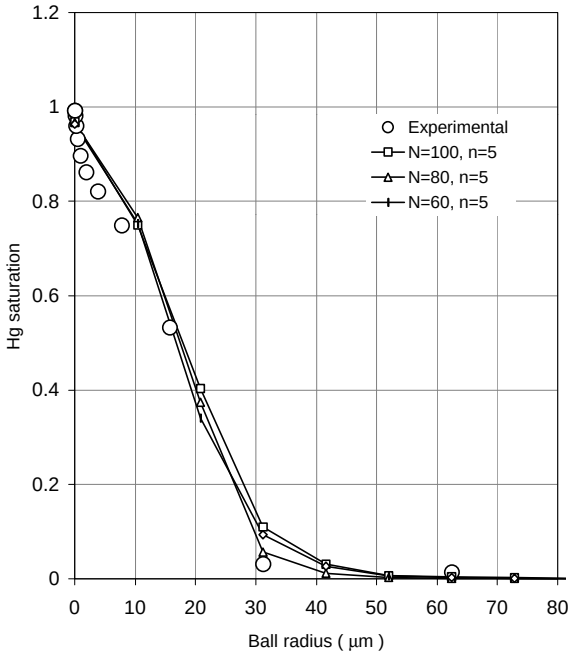

Figure 10. Comparison of simulation results with experimental data for Berea 500 mD sandstone.

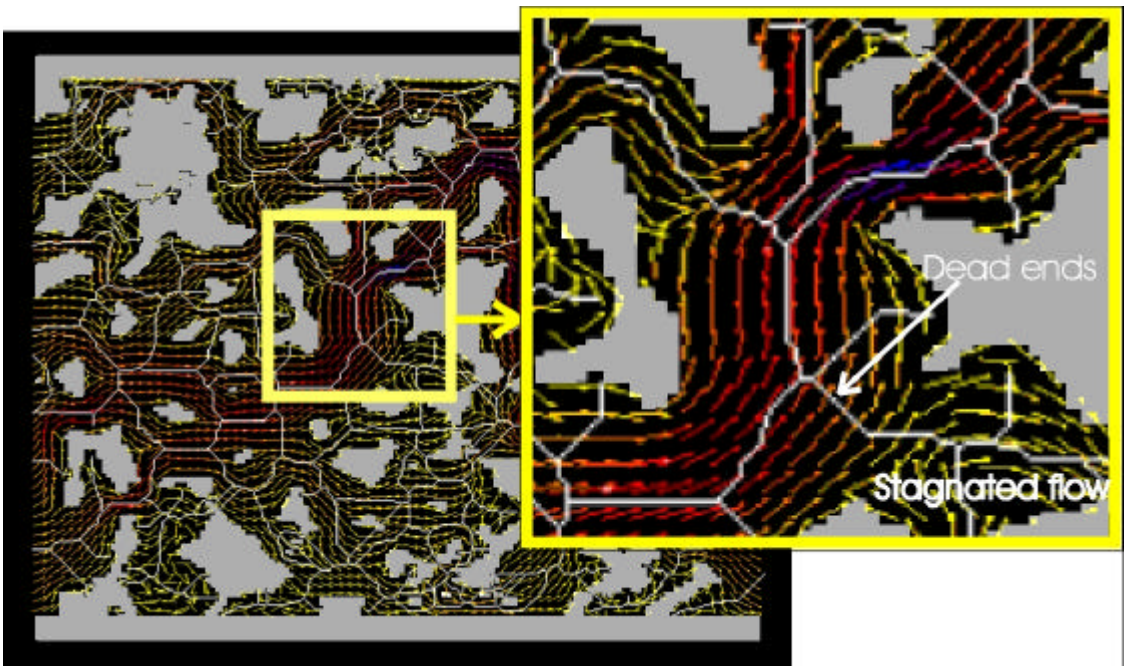

Figure 11. 2-D skeleton of the pore space superposed to the local velocity field, illustrating a geometrical region where flow is stagnated, presenting a low speed vortex.

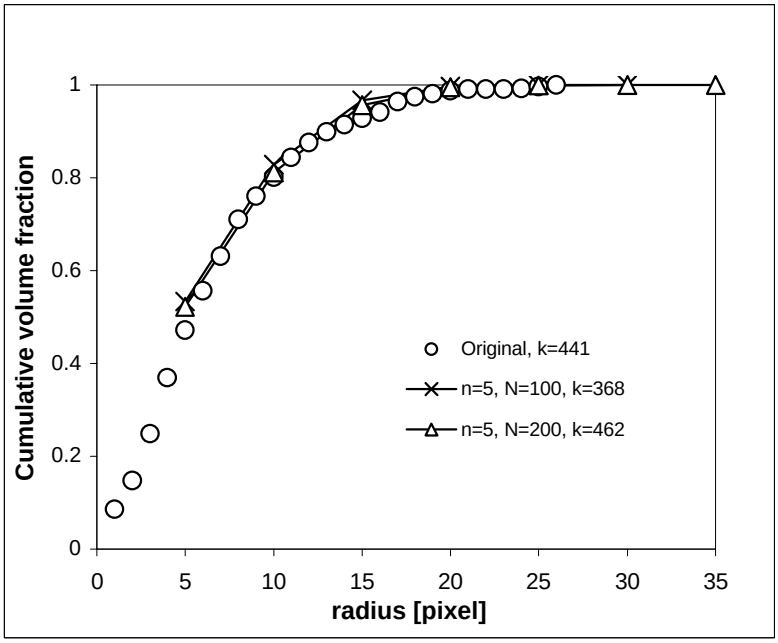

Figure 12. Pore size distribution and predicted LGA permeability values for a typical Brazilian sandstone. Experimental value measured at CENPES/Petrobras was k=441 mD.

Table 1. Comparison of the result for Berea sandstone 500 mD for different sampling factors n and linear size N. Table also shows the number of skeleton nodes where pressure is to be calculated in the simulation.

n	N	Node numbers	K (mD)
4	60	2,098	169.1
	80	5,187	181.4
	100	10,957	226.4
	120	19,323	335.7
5	40	697	209.4
	100	13,125	465.4
	110	18,390	478.3
	120	24,805	432.9
	150	48,422	452.2
6	40	745	362.5
	60	2,748	433.7
	80	6,897	440.1
	100	14,197	439.4
	120	25,300	459.5
8	30	327	933.5
	40	909	946.8
	60	3,490	928.3